Collision dynamics of a liquid fire suppressant upon a heated wax surface

Manzello S.L., Yang J.C.

Building and Fire Research Laboratory, National Institute of Standards and Technology (NIST), Gaithersburg, MD 20899-8662 USA, corresponding author: samuel.manzello@nist.gov

The impact of a distilled water droplet upon a heated wax surface was investigated experimentally using a high-speed digital camera at 1000 frames/s. Two different droplet impact Weber numbers (*We*) were considered and the collision dynamics were investigated with the temperature of the wax surface varied from 20 ºC to 75 ºC. For each impact *We* number, the evolution of the liquid film diameter was measured as a function of surface temperature. At *We* = 27, the evolution of the liquid film diameter displayed three distinct regimes: spreading, retraction, and secondary spreading. The liquid film diameter was observed to recoil faster as the surface temperature of the wax was increased. The increase in recoil speed was accompanied by a reduction in the effective Ohnesorge number (*Oh*). At *We* = 150, as the droplet recoiled, an unstable column of fluid was observed to rise above the wax surface. The instability of the fluid column at *We* = 150 was explained using Rayleigh instability theory. At 75 ºC, the melting point of the wax, collision dynamics were qualitatively similar to droplet impact on a liquid surface.

1. Introduction

Liquid droplet interaction with a surface has been studied for more than a century [1]. Fundamental understanding of droplet/surface interaction is important in agricultural applications, atmospheric sciences, criminal forensics, and fire suppression. The characteristics of the droplet/surface interactions depend upon the properties of the droplet, the impacted surface, impact velocity, geometry, and the medium (liquid, gas, dispersion) through which the droplet traverses prior to impact [2].

A crucial distinction in liquid droplet/surface interaction investigations is the type of impacted surface. In a broad sense, the target surface can be classified as either a solid or a liquid surface. The collision dynamics of the impinging droplet can be vastly different for liquid and solid surfaces [2]. The fluid mechanics of droplet collision with a solid surface has been studied under a variety of conditions [3-10]. Droplet collision with liquid surfaces has been studied in some detail as well [11-20]

The impact of a liquid droplet with a solid surface can result in the droplet spreading, splashing, or rebounding on a solid surface whereas the impact of a liquid droplet with a liquid surface can result in the droplet floating, bouncing, coalescing, and splashing on the liquid surface [2]. Most, if not all, of the droplet impact literature has considered droplet impingement on either a solid or liquid surface. In the present work, droplet/surface interaction was performed using distilled water droplets and a wax surface. A wax surface was selected since it allows the observation of droplet collision dynamics on a surface that changes its properties as the temperature is increased. For low surface temperatures, impact will occur on a solid surface. As the surface temperature is raised, the wax will soften, affording the investigation of droplet impact on a gradually yielding surface. Droplet/surface interaction on a heated wax surface is of importance to fire suppression as it may be considered a *first-step* to understand how a liquid fire suppressant would behave when impinging upon a burning surface that changes it properties with temperature

(*e.g.* polymeric surface).

2. Experimental Description

Figure 1 is a schematic of the experimental setup which includes the droplet generator, target surface, heating element, and imaging system. Droplets were generated using a syringe pump programmed to dispense the liquid at a rate of 0.001 mL/s. The droplet was formed at the tip of the needle (22 gauge), and detached from the syringe under its own weight. The temperature of the impinging droplets were fixed at 20 °C. The wax, which was contained in a glass cylinder, was heated by placing the container on a copper block with two miniature cartridge heaters embedded within it. The temperature of the block was measured using a thermocouple embedded within the surface. The temperature was controlled within to ± 1 °C using a temperature controller. The imaging system used to capture droplet impingement dynamics, as well as the image processing methodology to obtain droplet velocity and droplet diameter, has been described in detail elsewhere [7,8].

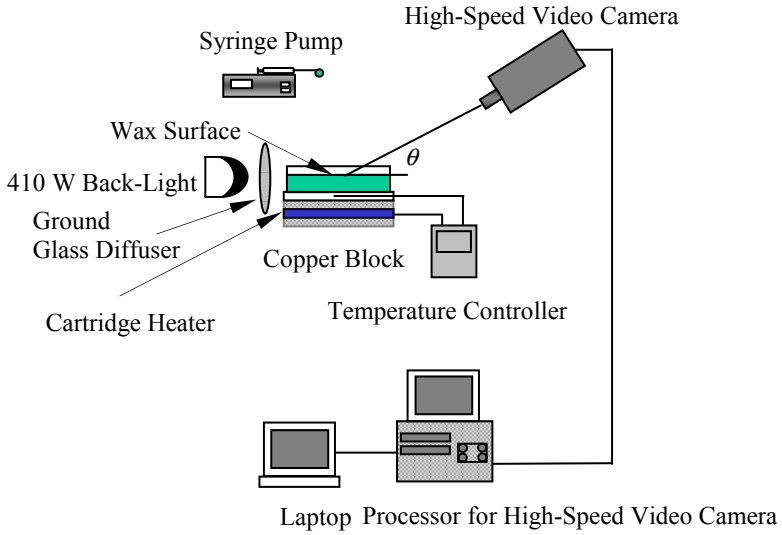

Fig. 1 Schematic of experimental setup

A commercial paraffin wax was used for the experiments. This type of wax was observed to have a melting point of approximately 75 ºC. To prepare the wax surface, pieces of solid wax were placed in a glass cylinder, 125 mm in diameter. The glass cylinder was heated on a hot plate to melt the wax. Wax pieces were added until a 10 mm pool of molten wax filled the glass cylinder. The pool of molten wax was then allowed to solidify by cooling for 8 h prior to performing droplet impingement experiments.

3. Results and Discussion

Figure 2a displays temporally resolved images of distilled water droplet impingement upon a wax surface at 20 °C, 70 °C, and 75 ºC for an impact Weber number of 27. The Weber number, the ratio of kinetic energy to surface energy of the droplet, is defined as $We = \rho D V^2/\sigma$, where ρ is the density, D is the initial droplet diameter, V is the impact velocity, and σ is the surface tension. Since each experiment displayed similar qualitative trends, results of three consecutive experiments

were used for data analysis. The relative standard uncertainty in determining the *We* number was ± 8 %. At 20 ºC, the droplet impacted, and spread upon the surface. The liquid film then began to recoil, and ultimately produced a near vertical column of fluid on the surface. The column of fluid ultimately collapsed upon the surface. As the surface temperature was raised, qualitatively similar collision dynamics were observed until the melting temperature was approached.

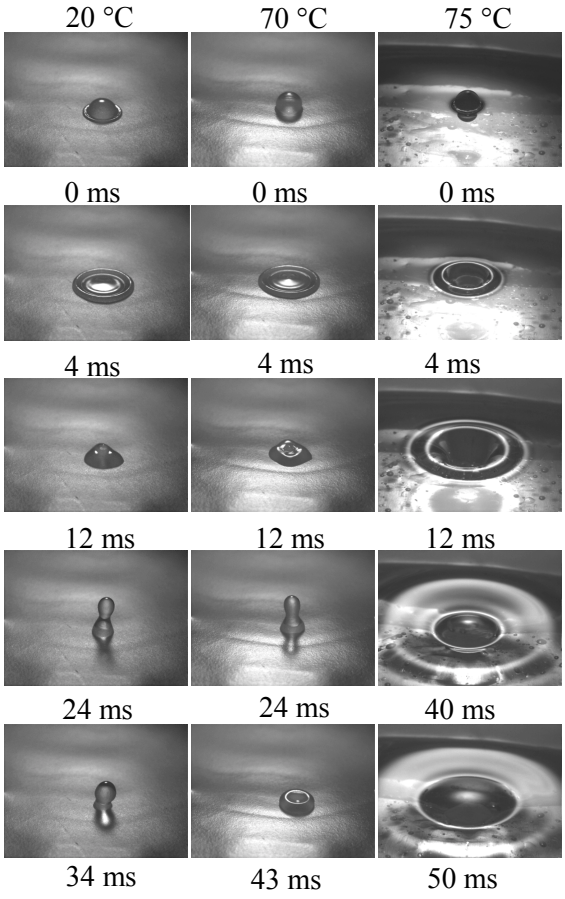

Fig. 2a *We* = 27

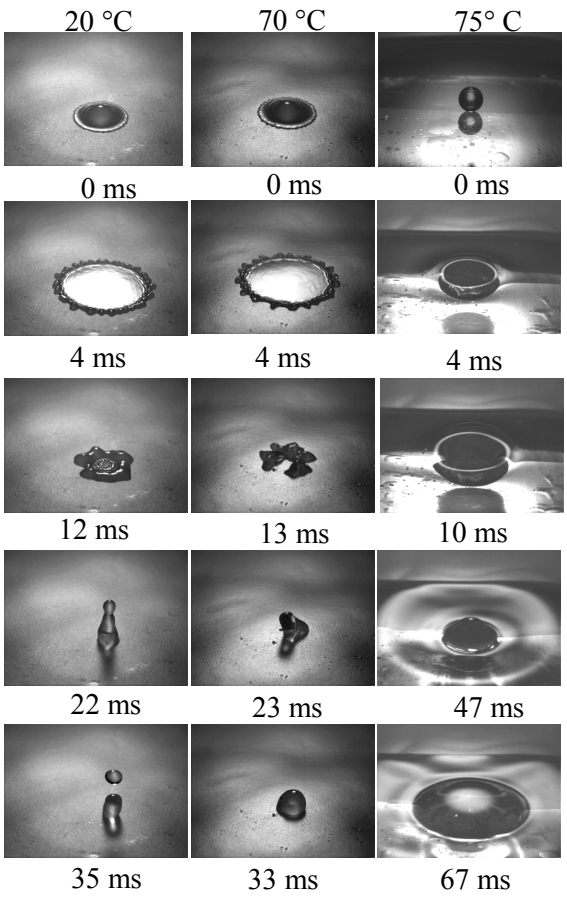

Fig.2b *We* =150

At 75 ºC, the approximate melting point of the wax, dramatic differences were observed. At this temperature, a phase transition occurred in the wax. The water droplet no longer makes contact with a solid surface, rather the droplet impacted upon a molten wax surface. A crater was formed, and the crater continued to penetrate into the molten liquid until a time of ≈ 16 ms. As the crater began to rise from the liquid surface, a small jet appeared.

The collision dynamics are displayed in figure 2b for water droplet impingement upon the wax surface for an impact *We* number of 150. The *We* number was varied by increasing the height of the syringe pump from the surface. For impact at *We* = 150 with a surface temperature of 20 ºC, the droplet spread over the wax surface and rebounded. The cylindrical column of fluid became unstable and a droplet was pinched off at the tip. At a surface temperature of 70 ºC and *We* = 150, the dynamics were similar to *We* = 27, namely the column of fluid formed after rebound did not breakup.

For droplet impingement upon the molten wax surface (75 ºC) at *We* = 150, a more pronounced crater was observed after impact. The depth of the crater penetrated the liquid surface,

and a larger jet was observed to emanate from the crater. The crater and jet dynamics were affected as the impact *We* number was increased (*cf*. Fig. 2a and Fig. 2b).

Clearly, the column of fluid formed after the droplet rebounded was unstable at *We* = 150. A vast amount of literature is available regarding liquid jet breakup due to instability [21,22]. These studies have focused on the breakup of a liquid jet comprised of a single fluid emanating from a nozzle into a quiescent gas. These analyses were extrapolated to the present experiments by assuming that the column of fluid that rises above the wax surface is similar to a jet emanating from a nozzle. Thus, the term jet and liquid column of fluid on the wax surface will be used interchangeably.

Reitz and Bracco [23] delineated jet breakup into four different regimes, Rayleigh regime, wind-induced regime, second wind regime, and the atomization regime. The type of breakup observed in the present experiments is not characteristic of very high jet velocities (*i.e*. second wind and atomization regime). Rather, it is assumed that liquid jet breakup occurred within the Rayleigh breakup regime. Within the Rayleigh breakup regime, the size of the droplets pinched off from the jet are on the order, or larger, than the jet diameter. Such behavior was observed in the present experiments. For the Rayleigh breakup regime, the breakup length of the jet scales linearly with the jet velocity [22]. Thus, a jet with a given velocity must reach a certain length before droplets can be pinched off from the jet. The velocity of the jet issuing from the wax surface was estimated from the images of the collision dynamics. At 20 ºC, 40 ºC, and 60 ºC, the velocity of the jet rising from the wax surface at *We* = 150 pool is considerably higher than the velocity of the jet rising from the wax surface at *We* = 27. For example, for *We* = 27, and *We* =150 at 20 ºC, the jet velocity was estimated to be 0.25 m/s ± 0.027 m/s, and 0.35 m/s ± 0.04 m/s, respectively (mean ± standard deviation). The lower velocity of the water jet at *We* = 27 suggests that the jet velocity is too low to reach the necessary breakup length. This increase in jet velocity may be the reason why the column of fluid is able to separate at *We* = 150.

The increase in jet velocity at high *We* number is due to the fact that the droplet spreads more at high *We* number [24]. When the liquid film spreads further, it is able to recoil faster, due to the larger driving force between the maximum liquid film diameter and the equilibrium value.

At 70 ºC, however, the column of fluid *did not* become unstable at *We* = 150. The reason for this is due to differences in surface roughness. The wax began to make a phase transition from solid to liquid at 70 ºC. Closer inspection of the surface at 70 ºC revealed small bumps on the surface. At 70 ºC, the enhanced roughness of the surface affected the ability of the liquid film to regroup, and form a liquid column (jet). This resulted in a lower jet velocity, in effect precluding breakup of the jet at 70 ºC.

Disturbances were observed along the periphery of the liquid film at *We* = 150. Such disturbances were not observed at *We* = 27. As the droplet impacts the surface, the liquid film formed spreads radially outward and the fluid experiences a large deceleration due to retardation by viscous forces. Allen [25] believed this decelerating interface results in a Rayleigh-Taylor instability, namely an instability that exists when an interface of two different fluids is accelerated towards the fluid of higher density [26]. The Rayleigh-Taylor instability results in an interfacial wave along the edge of the expanding liquid film.

Thoroddsen and Sakakibara [27] investigated the disturbances along the periphery of the spreading liquid film as well. Based on experimental observations, they believed that the disturbances are the result of a Rayleigh-Taylor instability, but the source of the instability is different than the one purported by Allen [25]. Namely, the instability is the result of a fluid ring that decelerates before making contact with the bottom of the solid surface. Although debate exists

in the literature about the exact cause of the Rayleigh-Taylor instability, the present experiments demonstrate that these instabilities exist for droplet impingement on a wax surface at *We* = 150, and do not seem to be influenced markedly by changes in surface temperature.

The evolution of the non-dimensional liquid film diameter with time was measured as a function of temperature for *We* = 27, and *We* = 150, and is displayed in figure 3. Such measurement is important in fire suppression as it quantifies the portion of surface undergoing cooling. The non-dimensional liquid film diameter was defined as, $\beta = d/D$, where d is the instantaneous liquid film diameter. The non-dimensional liquid film diameter was obtained from the average of three measurements at each temperature, with the error bars representing the standard deviation. For low impact *We* number, the liquid film diameter was measured up to time it reached its equilibrium value (*i.e*. shape of sessile droplet on wax surface). For impact at *We* = 150, the liquid film diameter was measured up to time the droplet detached from the column of fluid. Due to the phase transition that was observed to occur, the non-dimensional liquid film diameter was not measured at 70 ºC for *We* = 27, and *We* = 150.

Three distinct regimes were observed for impact at *We* = 27. After droplet impact, the liquid film expanded to a maximum value. The liquid film began to recoil, and reached a minimum value. The minimum value corresponded to the time of the maximum extension of the liquid column of fluid on the surface. With the collapse of the liquid column, the liquid film once again increased in magnitude, and then recoiled again, and reached the final equilibrium value

These observations were in qualitative agreement with previous investigations on wax surfaces at 20 ºC [6,28,29]. Ford and Furmidge [28] considered water droplet impact at 20 ºC on a beeswax surface. A continuous stream of droplets was generated using a vibrating blade generator, and the droplets fell onto a slowly rotating surface containing beeswax. The collision dynamics were photographed using a stroboscopic lamp. They observed three distinct stages in the evolution of film diameter: initial spreading, retraction, and secondary spreading. Fukai *et al*. [29] performed water droplet impact experiments on a commercial wax surface and measured the non-dimensional liquid film diameter at 20 ºC. They reported qualitatively similar behavior to Ford and Furmidge [29]. Neither investigator considered the influence of temperature on the collision dynamics.

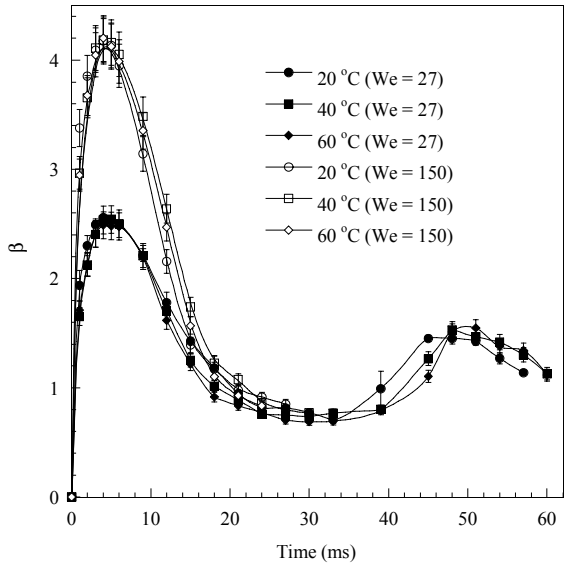

Fig. 3 Measured non-dimensional liquid film diameter as a function of time.

At impact *We* = 150, the non-dimensional liquid film diameter expanded to a maximum and then recoiled (see figure 3). However, ≈ 30 ms, the liquid column became unstable, and a droplet was pinched off from the surface, precluding further measurement of the liquid film diameter. At *We* = 150, the liquid film diameter was larger than that at *We* = 27.

Several correlations are available to calculate the maximum non-dimensional spread diameter within the film evaporation regime. In a recent review by Healy *et al*. [30], seven correlations were tested using a variety of experimental data available in the literature. It was reported that the Kurabayashi-Yang correlation provided the best agreement between the prediction and measured $\beta_{\max}$ for data in the film evaporation regime. Manzello and Yang [8] also reported good agreement for water droplet impact on polished stainless steel surfaces within the film evaporation regime using the Kurabayashi-Yang correlation. The Kurabayashi-Yang correlation, provided in Yang [31], is given as:

$$\frac{We}{2} = \frac{3}{2}(\beta_{\max})^2 \left[1 + \frac{3We}{\mathrm{Re}} \left((\beta_{\max})^2 Ln(\beta_{\max}) - \frac{(\beta_{\max})^2 - 1}{2} \right) \left(\frac{\mu}{\mu_{wall}} \right)^{0.14} \right] - 6 \quad (1)$$

where $\beta_{max} = d_{max}/D$, μ is the dynamic viscosity, μ_{wall} is the dynamic viscosity evaluated at the wall temperature, and $\mathrm{Re} = \rho DV/\mu$. The Kurabayashi-Yang equation was obtained based upon an energy balance between the initial condition, and the final, fully spread condition, and is valid up to the saturation temperature of pure water. The comparison between the measured non-dimensional liquid film diameter and the predicted values at 20 ºC are displayed in table I. Overall, the correlation provided better agreement at higher impact *We* number.

To investigate the influence of surface temperature on droplet recoil, the recoil speed was measured as a function of temperature for impact at *We* = 27. The recoil speed was defined as the average velocity of the liquid film diameter from its maximum extension to the time the liquid film diameter passed through the equilibrium value [24]. The recoil speed increased as the surface temperature was increased. For example, at 20 ºC and 60 ºC, the recoil speed was measured to be 0.3 m/s ± 0.03 m/s and 0.4 m/s ± 0.02 m/s, respectively (mean ± standard deviation). The recoil speed was not measured for impact at *We* = 150 since the equilibrium value of the droplet could not be determined due to jet breakup (*i.e*. two droplets appeared on the surface after the collision dynamics ended).

We	$\beta_{\mathrm{max,measured}}$	$\beta_{\mathrm{max,\ predicted}}$
27	2.5	3.2
150	4.0	4.5

Table I Comparison of measured and predicted maximum non-dimensional liquid film diameter

The initial spreading of the droplet on the surface is governed by the impact *We* number, whereas the Ohnesorge number and contact angle govern the recoil stage [24]. The Ohnesorge (*Oh*) number, the ratio of the viscous force to surface tension force, is defined as $Oh = \mu/\sqrt{(\rho D\sigma)}$, and is a measure of the resisting force during recoil. Kim and Chun [24] reported that for fixed impact energy (fixed *We* number), the initial spreading processes were almost identical, yet the recoiling was dependent on the *Oh* number. In the present experiments, at *We* = 27, the maximum value of the non-dimensional liquid film diameter was nearly identical with temperature, yet the recoil speed increased with temperature. The increase in recoil speed with an attendant increase in surface

temperature may be due to the decrease in *Oh* number. To evaluate the effective *Oh* number, the liquid properties were evaluated at a film temperature, $(T_s+T_l)/2$, where T_s and T_l are the surface and liquid droplet temperature, respectively. For water, the dynamic viscosity, density, and surface temperature decrease with temperature. It may be expected that as temperature is increased, both the numerator and denominator in the *Oh* number would decrease, allowing the *Oh* number to remain relatively constant. Based on the computations, however, the *Oh* decreased over the range of temperatures considered. The values of *Oh* number were $2.2\text{x}10^{-3}$, $1.7\text{x}10^{-3}$, and $1.4\text{x}10^{-3}$ at film temperatures of 20 ºC, 30 ºC, and 40 ºC, respectively. This is a consequence of the density and surface tension appearing under the radical. A lower *Oh* number at higher temperature suggests that the resisting force to droplet recoil is lower at higher temperature, which is confirmed by the experimental measurements.

At 75 ºC, the melting point of the wax, collision dynamics appeared to be qualitatively similar to droplet impact on a liquid surface [18,19]. At *We* = 27, a small jet was observed to form within the liquid with a more pronounced jet at *We* = 150. In the present study, however, the rheology of molten wax was not characterized. A comprehensive study of water droplet impingement upon molten wax would require rheology characterization as well as varying the pool depth of molten wax. Such questions are beyond the scope of this study.

4. Conclusions

For impact at *We* = 27, the evolution of the non-dimensional liquid film diameter displayed three distinct regimes: spreading, retraction, and secondary spreading. The liquid film diameter was observed to recoil faster as the surface temperature was increased. The increase in recoil speed was accompanied by a reduction in the effective *Oh* number. At *We* = 150, instabilities were observed along the periphery of the spreading liquid film. The instability of the liquid column at *We* = 150 was explained using Rayleigh instability theory. At 75 ºC, the melting point of the wax, collision dynamics appeared to be qualitatively similar to droplet impact on a liquid surface.

5. Acknowledgments

SLM acknowledges partial financial support from a National Research Council (NRC) Post-Doctoral Fellowship. This paper is an official contribution of the National Institute of Standards and Technology not subject to copyright in the United States.

6. References

1. Reynolds, O., *Proc. Manchester Lit. Phil. Soc*. **21** (1881) 1-2.
2. Rein, M.J., *Fluid Dyn. Res.* **12** (1993) 61-93.
3. Engel, O.G., *J. Res. NBS* **5** (1955) 281-298.
4. Chandra, S., Avedisian, C.T., *Proc. Roy. Soc. Lond. A* **432** (1991) 13-41.
5. Bernardin, J.D., Stebbins, C.J., Mudawar, I., *Int. J. Heat Mass Trans*. **40** (1997) 247-267.
6. Rioboo, R., Morengo, M., Tropea, C., *Exp. Fluids* **33** (2002) 112-124.
7. Manzello, S.L.,Yang, J.C., *Int. J. Heat Mass Trans.* **45** (2002) 3961-3971.
8. Manzello, S.L.,Yang, J.C., *Proc. Roy. Soc. Lond. A* **458** (2002) 2417-2444.
9. Manzello, S.L., Yang, J.C., *J. Colloid Interface Sci*. **256** (2002) 418-427.
10. Haferl, S., Poulikakos, D., *Int. J. Heat Mass Trans*. **46** (2003) 535-550.
11. Thompson, J.J., Newall, H.F., *Proc. Roy. Soc. Lond.* **39** (1885) 417-436.

12. Worthington, A.M., A Study of Splashes, Longmans, Green and Company, 1908.
13. Macklin, W.C., Hobbs, P.V., *Science* **166** (1969) 107-108.
14. Rodriguez, F., Mesler, R.J., *J. Colloid Interface Sci.* **106** (1985) 347-352.
15. Hsiao, M., Lichter, S., Quintero, L., *Phys. Fluids* **31** (1988) 3560-3562.
16. Rein, M.J., *J. Fluid Mech*. **306** (1996) 145-165.
17. Wang, A.B., Chen, C.C., *Phys. Fluids* **12** (2000) 2155-2158.
18. Manzello, S.L.,Yang, J.C., *Expt. Fluids* **32** (2002) 580-589.
19. Manzello, S.L.,Yang, J.C., *Phys. Fluids* **15** (2003) 257-260.
20. Manzello, S.L.,Yang, J.C., Cleary, T.G., *Fire Safety J*. (2003) in press.
21. Rayleigh, J.W.S., *Proc. Roy. Soc. Lond.***34** (1882) 130-145.
22. Lin, S.P., Reitz, R.D., *Annu. Rev. Fluid Mech*. **30** (1998) 85-105.
23. Reitz, R.D., Bracco, F.V., Mechanisms of breakup of round liquid jets, The encyclopedia of fluid mechanics, Gulf, Houston, 1986.
24. Kim, H.Y., Chun, J.H., *Phys. Fluids* **13** (2001) 643-659.
25. Allen, R.F., *J. Colloid Interface Sci.* **51** (1975) 350-351.
26. Taylor G.I., *Proc. Roy. Soc. Lond. A* **201** (1950) 192-196.
27. Thoroddsen, S.T., Sakakibara, J., *Phys. Fluids* **10** (1998)1359-1378.
28. Ford, R.E., Furmidge, C.G.L., (1967) *Wetting, Soc. Chem. Industry* **25** (1967) 417-432.
29. Fukai, J., Shiba, Y.,Yamamoto, T., Miyatake, O., Poulikakos, D., Megaridis, C.M., Zhao, Z., *Phys. Fluids* **7** (1995) 236-247.
30. Healy, W.M., Hartley, J.G., Abdel-Khalik, S.I., *Int. J. Heat Mass Trans*. **39** (2001) 3079-3082.
31. Yang, W.J., Technical Report 535, Institute of Space and Aeronautical Science, University of Tokyo, 1975.